

MOVE BEYOND THE THRESHOLD

As an extended half-life recombinant FVIII, Esperoct[®] offers a simple way to reach higher trough FVIII activity levels compared to standard half-life treatments.^{**1,4-10}

Mode of Action Video
Click here

In adults and adolescents[†] with severe haemophilia A, Esperoct[®] demonstrated:

A simple, fixed starting dose:^{1,4}
50 IU/kg every 4 days

Higher trough FVIII activity levels vs. SHL treatments:^{1,4-10}
Mean trough FVIII activity levels of 3%

Low ABR:^{1,4}
Median total ABR[‡] of 1.18

*40°C storage for up to 3 months before reconstitution¹ **Esperoct[®] is licenced for the treatment and prophylaxis of bleeding in patients 12 years and above with haemophilia A (congenital factor VIII deficiency)¹

This advertisement is intended for Healthcare Professionals

THE ONLY EHL FVIII^{rFVIII} STABLE UP TO 40°C

Prescribing Information

Esperoct[®]

Esperoct 500 IU Esperoct 1000 IU Esperoct 1500 IU Esperoct 2000 IU Esperoct 3000 IU (powder and solvent for solution for injection) Turoctocog alfa pegol. Human factor VIII, produced by recombinant DNA technology in a Chinese Hamster Ovary (CHO) cell line, and no additives of human or animal origin are used in the cell culture, purification, conjugation or formulation. **Indication:** Treatment and prophylaxis of bleeding in patients 12 years and above with haemophilia A (congenital factor VIII deficiency) **Posology and administration:** The dose, dosing interval and duration of the substitution therapy depend on the severity of the factor VIII deficiency, on the location and extent of the bleeding, on the targeted factor VIII activity level and the patient's clinical condition. **On demand treatment and treatment of bleeding episodes:** Required dose IU = body weight (kg) x desired factor VIII rise (%) (IU/dL) x 0.5 (IU/kg per IU/dL). **Mild haemorrhage:** early haemarthrosis, mild muscle bleeding or mild oral bleeding. Factor VIII level required (IU/dL or % of normal): 20-40. Frequency of doses: 12-24, until the bleeding is resolved. **Moderate haemorrhage:** More extensive haemarthrosis, muscle bleeding, haematoma. Factor VIII level required (IU/dL or % of normal): 30-60. Frequency of doses: 12-24, until the bleeding is resolved. **Severe or life-threatening haemorrhages:** Factor VIII level required (IU/dL or % of normal) – 60-100. Frequency of doses: 8-24, until the threat is resolved. **Perioperative management: Minor surgery including tooth extraction.** Factor VIII level required (IU/dL or % of normal): 30-60. Frequency of doses (hours): within one hour before surgery; repeat after 24 hours if necessary. Duration of therapy: single dose or repeat injection every 24 hours for at least 1 day until healing is achieved. **Major surgery:** Factor VIII level required (IU/dL or % of normal): 80-100 (pre- and post-operative). Frequency of doses (hours): Within one hour before surgery to achieve factor VIII activity within the target range. Repeat every 8 to 24 hours to maintain factor VIII activity within the target range. Repeat injection every 8 to 24 hours as necessary until adequate wound healing is achieved. Consider continuing therapy for another 7 days to maintain a factor VIII activity of 30% to 60% (IU/dL). **Prophylaxis:** The recommended starting dose is 50 IU of Esperoct per kg body weight every 4 days. The maximum single dose is 75 IU/kg. Adjustments of doses and administration intervals may be considered based on achieved factor VIII levels and individual bleeding tendency. **Paediatric population:** The dose in adolescents (12 years and above) is the same as for adults. In children below 12 years long-term safety has not been established. **Method of administration:** Intravenous injection (over approximately 2 minutes) after reconstitution of the powder with 4 mL supplied solvent (sodium chloride 9 mg/mL (0.9%) solution for injection). **Contraindications:** Hypersensitivity to the active substance or to any of the excipients, or to hamster protein. **Special warnings and precautions for use:** **Hypersensitivity:** Allergic-type hypersensitivity reactions are possible due to traces of hamster proteins, which in some patients may cause allergic reactions. If symptoms of hypersensitivity occur, patients should be advised to immediately discontinue the use of the medicinal product and contact their physician. Patients should be informed of the early signs of hypersensitivity reactions including hives, generalised urticaria, tightness of the chest, wheezing, hypotension, and anaphylaxis. In case of shock, standard medical treatment for shock should be implemented. **Inhibitors:** The formation of neutralising antibodies (inhibitors) to factor VIII is a known complication in the management of individuals with haemophilia A. These inhibitors are usually IgG immunoglobulins directed against the factor VIII pro-coagulant activity, which are quantified in Bethesda Units (BU) per ml of plasma using the modified assay. The risk of developing inhibitors is correlated to the severity of the disease as well as the exposure to factor VIII, this risk being highest within the first 50 exposure days but continues throughout life although the risk is uncommon. The clinical relevance of inhibitor development will depend on the titre of the inhibitor, with low titre posing less of a risk

of insufficient clinical response than high titre inhibitors. Patients treated with coagulation factor VIII products should be monitored for the development of inhibitors by appropriate clinical observations and laboratory tests. If the expected factor VIII activity plasma levels are not attained, or if bleeding is not controlled with an appropriate dose, testing for factor VIII inhibitor presence should be performed. In patients with high levels of inhibitor, factor VIII therapy may not be effective and other therapeutic options should be considered. **Cardiovascular events:** In patients with existing cardiovascular risk factors, substitution therapy with factor VIII may increase the cardiovascular risk. **Catheter-related complications:** If a central venous access device (CVAD) is required, the risk of CVAD-related complications including local infections, bacteraemia and catheter site thrombosis should be considered. **Paediatric population:** Listed warnings and precautions apply both to adults and adolescents (12-18 years). **Excipient-related considerations:** Product contains 30.5 mg sodium per reconstituted vial, equivalent to 1.5% of the WHO recommended maximum daily intake of 2.0 g sodium for an adult. **Fertility, pregnancy and lactation:** Animal reproduction studies have not been conducted with factor VIII. Based on the rare occurrence of haemophilia A in women, experience regarding the use of factor VIII during pregnancy and breast-feeding is not available. Therefore, factor VIII should be used during pregnancy and lactation only if clearly indicated. **Undesirable effects:** The Summary of Product Characteristics (SmPC) should be consulted for a full list of side effects. **Common** ($\geq 1/100$ to $< 1/10$): Rash, erythema, pruritus, injection site reactions. **Uncommon** ($\geq 1/1,000$ to $< 1/100$): Factor VIII inhibition, hypersensitivity. **MA numbers and Basic NHS Price:** Esperoct 500 IU EU/1/19/1374/001 £425 Esperoct 1000 IU EU/1/19/1374/002 £850 Esperoct 1500 IU EU/1/19/1374/003 £1,275 Esperoct 2000 IU EU/1/19/1374/004 £1,700 Esperoct 3000 IU EU/1/19/1374/005 £2,550 **Legal category:** POM. **For full prescribing information please refer to the SmPC** which can be obtained from: Novo Nordisk Limited, 3 City Place, Beehive Ring Road, Gatwick, West Sussex, RH6 0PA. **Marketing Authorisation Holder:** Novo Nordisk A/S, Novo Allé, DK-2880 Bagsværd, Denmark. **Date last revised:** March 2020

Esperoct[®] is a trademark owned by Novo Nordisk Health Care AG, Switzerland.

Adverse events should be reported. Reporting forms and information can be found at www.mhra.gov.uk/yellowcard or search for MHRA Yellow Card in the Google Play or Apple App Store. Adverse events should also be reported to Novo Nordisk Limited (Telephone Novo Nordisk Customer Care Centre 0845 6005055). Calls may be monitored for training purposes.

ABR, annualised bleed rate; EHL, extended half-life; FVIII, factor VIII; rFVIII, recombinant factor VIII; SHL, standard half-life

[†]Previously treated patients, 12 years and above¹

[‡]Total ABR includes all bleeds: spontaneous, traumatic and joint bleeds⁴

References: 1. Esperoct[®] Summary of Product Characteristics. 2. Adynovi[®] Summary of Product Characteristics. 3. Elocta[®] Summary of Product Characteristics. 4. Giangrande P et al. Thromb Haemost 2017; 117:252–261. 5. Tiede A et al. J Thromb Haemost 2013; 11:670–678. 6. Advate[®] Summary of Product Characteristics. 7. Kogenate[®] Summary of Product Characteristics. 8. NovoEight[®] Summary of Product Characteristics. 9. Nuwiq[®] Summary of Product Characteristics. 10. Refacto AF[®] Summary of Product Characteristics.

Paediatric Burkitt lymphoma patient-derived xenografts capture disease characteristics over time and are a model for therapy

Sorcha Forde,¹ Jamie D. Matthews,¹
Leila Jahangiri,^{1,2} Liam C. Lee,¹
Nina Prokoph,¹ Tim I.M. Malcolm,¹
Olivier T. Giger,¹ Natalie Bell,³
Helen Blair,³ Aengus O'Marcaigh,⁴
Owen Smith,⁴ Lukas Kenner,^{5,6,7}
Simon Bomken,^{3,8,9}

Gladstone A. A. Burke^{10,*}  and
Suzanne D. Turner^{1,11,*} 

¹Division of Cellular and Molecular Pathology, Department of Pathology, University of Cambridge, Cambridge, ²Department of Life Sciences, Birmingham City University, Birmingham, ³Wolfson Childhood Cancer Research Centre, Translational and Clinical Research Institute, Newcastle University, Newcastle upon Tyne, UK, ⁴Children's Health Ireland at Crumlin, Dublin, Ireland, ⁵Department of Pathology, Medical University of Vienna, Vienna, ⁶Unit of Laboratory Animal Pathology, University of Veterinary Medicine Vienna, Vienna, ⁷Christian Doppler Laboratory for Applied Metabolomics, Vienna, Austria, ⁸The Great North Children's Hospital, The Newcastle upon Tyne Hospitals NHS Foundation Trust, Newcastle upon Tyne, ⁹Northern Institute for Cancer Research, Newcastle University, Newcastle upon Tyne, ¹⁰Department of Paediatric Oncology and Haematology, Addenbrooke's Hospital, Cambridge, UK, and ¹¹Central European Institute of Technology, Masaryk University, Brno, Czech Republic

Received 15 June 2020; accepted for publication 26 July 2020

Correspondence: Suzanne D. Turner, Division of Cellular and Molecular Pathology, Department of Pathology, University of Cambridge, Lab Block Level 3, BOX 231, Addenbrookes Hospital, Cambridge CB20QQ,

Summary

Burkitt lymphoma (BL) accounts for almost two-thirds of all B-cell non-Hodgkin lymphoma (B-NHL) in children and adolescents and is characterised by a *MYC* translocation and rapid cell turnover. Intensive chemotherapeutic regimens have been developed in recent decades, including the lymphomes malins B (LMB) protocol, which have resulted in a survival rate in excess of 90%. Recent clinical trials have focused on immunochemotherapy, with the addition of rituximab to chemotherapeutic backbones, showing encouraging results. Despite these advances, relapse and refractory disease occurs in up to 10% of patients and salvage options for these carry a dismal prognosis. Efforts to better understand the molecular and functional characteristics driving relapse and refractory disease may help improve this prognosis. This study has established a paediatric BL patient-derived xenograft (PDX) resource which captures and maintains tumour heterogeneity, may be used to better characterise tumours and identify cell populations responsible for therapy resistance.

Keywords: Burkitt lymphoma, patient derived xenograft, relapse, B-cell lymphoma, murine cancer models.

UK.

E-mail: sdt36@cam.ac.uk

*These authors contributed equally to this work.

B-cell non-Hodgkin lymphoma (B-NHL) represents the most common subtype of NHL in childhood and adolescence, accounting for up to 60% of all newly diagnosed lymphomas.^{1,2} Burkitt lymphoma (BL) alone accounts for almost two-thirds of B-NHL in children and adolescents and is most prominent in the 0–14 age group.³ The defining characteristic of BL is a translocation of the *MYC* oncogene on chromosome 8 with the immunoglobulin genes on chromosomes 14, 22 or 2 and it presents in advanced form (stage III/IV) in 70% of patients.^{4,5} In the modern era, all aggressive mature paediatric B-NHL patients receive the same treatment regimens and outcomes have improved dramatically in recent decades, with trials showing survival of approximately 90%.^{6–8} The clinical focus has been on establishing risk-stratification to reduce the acute and long-term toxicities associated with therapy for those patients with a favourable prognosis. Recent clinical trials in paediatric B-NHL involve the combination of rituximab, an anti CD20 antibody, with a chemotherapeutic backbone, based on the rationale that the CD20 antigen is present in over 98% of cases of paediatric mature B-NHL.⁹ The addition of rituximab to a modified lymphomes malins B (LMB) chemotherapy regimen has recently been evaluated in the Inter-B-NHL Ritux study with results showing prolonged event-free survival and overall survival among children and adolescents with high-grade, high-risk, mature B-NHL.¹⁰ Despite these developments, prognosis in refractory and relapse cases remains dismal, with few options to successfully salvage patients and the two-year overall survival rate with chemoimmunotherapy reported as 15–33%.^{11,12} The cellular population(s) responsible for propagating refractory/relapsed disease have not yet been identified, largely due to the lack of suitable model systems.¹³

Patient-derived xenograft (PDX) models have evolved as a powerful preclinical tool capable of bridging the gap between established cell lines and primary tumour samples. PDXs better maintain the heterogeneity of patient tumours and hence allow for a more clinically relevant examination of tumour evolution, response to therapy and development of chemo-resistance. Despite a relatively homogeneous histological appearance, studies have demonstrated both inter- (across patients) and intra- (within tumours) heterogeneity in BL.^{14,15} Love *et al.*¹⁶ reported considerable heterogeneity in the number of mutated genes across samples: out of a total of 70 mutated genes, the range of mutations in the sample cohort was 2 to 16. Model systems such as PDXs which capture the genetic and functional heterogeneity of primary paediatric BL will be necessary to identify targeted

therapies for individual patients, as well as to decipher the clonal dynamics that lead to resistant disease in 5–10% of patients.⁵ PDX models of B-cell lymphoma exist, although those published have been developed from adult tumours and consist mainly of the Diffuse Large B-cell Lymphoma (DLBCL) subtype, the most common B-cell lymphoma in the adult population, and their applicability to paediatric B-NHL is limited.¹⁷ This paper documents, to our knowledge, the establishment of the largest PDX resource for paediatric BL, providing a valuable tool to characterise tumours and better understand the functional and molecular characteristics of this tumour type.

Materials and methods

Primary patient samples

Paediatric B-NHL primary patient samples were obtained from redundant tissue taken at the time of the diagnostic biopsy, following informed consent on enrolment of patients to the Inter B-NHL Ritux clinical trial or following local ethical approval (Research Ethics Committee Reference: 07/q0104/16). One patient sample was obtained with informed consent from the Newcastle Haematology Biobank (Research Ethics Committee Reference: 07/H0906/109+5). One patient biopsy (to generate PDX6) was obtained at relapse from a drained peritoneal effusion of a patient refractory to ICE (ifosfamide, carboplatin, etoposide) therapy.

Patient sample processing

Mononuclear cells (MNCs) were isolated from pleural effusion, peripheral blood or bone marrow by gradient centrifugation over Lymphoprep™ (STEMCELL Technologies, Cambridge, UK). Tumour samples from solid biopsies underwent mechanical disaggregation by passing cells through a 70 µmol/l nylon cell strainer (BD Falcon, Erembodegem, Belgium) using the plunger of a 5 ml syringe (BD Plastipak, BD Falcon), applying light to medium mechanical force. Isolated MNCs were washed once with phosphate-buffered saline (PBS, ThermoFisher, Waltham, MA, USA) before injection into mice or further analysis.

Mice

JAX™ NSG Mice (NOD.Cg-Prkdc^{scid} Il2rg^{tm1Wjl}/SzJ) were obtained from Charles River, Margate, UK and housed in

individually ventilated cages (IVCs) under sterile pathogen-free (spf) conditions at the University of Cambridge under project licence numbers 80/2630 (2014–2017) and P4DBEFF63 (2018–2020). Additional animals in Newcastle were housed and used under project licence 60/4552 (2013–2018).

Tumour growth in NSG mice

Isolated MNCs (5×10^6) were suspended in 200 μ l of PBS and mixed with 200 μ l of matrigel (Corning, Flintshire, UK) before 300 μ l of suspension was injected subcutaneously (SC) or intraperitoneally (IP) into NSG mice. Once tumours reached the maximum regulatory allowed size of 1.2 cm (1.5 cm in 10% of cases) in any one direction, animals were culled and the tumour removed and disaggregated by passing cells through a 70 μ mol/l nylon cell strainer (BD Falcon). For serial passage, cells (1×10^5) were resuspended in matrigel as described and re-injected.

Fluorescence in situ hybridization

Fluorescent *in situ* hybridization (FISH) was carried out to determine the presence of the *MYC* translocation. Single-cell suspensions were collected by centrifugation at 200 g for 5 min and resuspended in Carbonyl's Fixative (3:1 methanol:glacial acetic acid). FISH was performed using a Vysis LSI IGH/*MYC*/CEP 8 Tri-Color Dual Fusion Probe Kit (Abbott Diagnostics, Maidenhead, UK). Results were reported as the percentage of cells positive for *IGH*–*MYC* rearrangement as well as the signal pattern.

Tumour histology

Following extraction of tumours, either the whole tumour or a representative biopsy was immediately placed in 10% neutral-buffered formalin (Sigma-Aldrich, Gillingham, UK). After 24 h the tumour was removed and placed in 70% ethanol/PBS. Tumours were embedded in paraffin before sections were cut and stained with haematoxylin and eosin using standard procedures. Sections were analysed by a histopathologist at the Department of Pathology, University of Cambridge and images captured at 20 \times magnification.

Flow cytometry

Cells were washed with PBS and collected by centrifugation at 250 g for 5 min before resuspension in flow cytometry buffer [PBS, 0.05% Bovine Serum Albumin (ThermoFisher, Waltham, MA, USA)] at a concentration of 1×10^6 cells/ml. Cell suspension (100 μ l) was added to each well of a 96-well plate and stained with the following: murine phycoerythrin, fluorescein isothiocyanate, allophycocyanin or cyanine 7 (Cy7)—conjugated antibodies: CD9, CD10, CD19, CD20, CD21, CD24, CD27, CD34, CD38, CD40, CD44, CD45, CD49d, CD49f, CD59, CD90, CD117, CD133, CD184, ABCG2 (BD

Biosciences, Erembodegem, Belgium). After staining (40 min at 4°C, 1:100), cells were washed in PBS and resuspended in 2 ml of flow cytometry buffer before immediate analysis on a BD Accuri C6 or a LSR Fortessa Flow Cytometer. At least 10 000 events were recorded and data analysed with FlowJo v9.1 (BD, Erembodegem, Belgium). The lymphocyte population was selected and expression levels determined based on gates set using unstained control.

Whole genome sequencing

DNA was extracted with a DNeasy Blood & Tissue Kit (Qiagen, Manchester, UK) and whole genome sequencing (WGS) was performed on the Illumina Novaseq 6000 (Cambridge, UK). Sequencing reads in FASTQ format were quality-checked with FastQC (version 0.11.9; Babraham Bioinformatics, Cambridge, UK, <https://www.bioinformatics.babraham.ac.uk/projects/fastqc/>) and mapped to the hg38 human genome assembly using BWA (0.7.17-4, Heng Li, Boston, MA, USA, <https://github.com/lh3/bwa>) with the '-M' compatibility option. BAM files were coordinate-sorted with Samtools (1.10.3, Genome Research Limited, Saffron Walden, UK, <http://www.htslib.org/>). Duplicate marking and base quality score recalibration was performed with the GATK suite (4.1.4.0, Broad Institute, Cambridge, MA, USA, <https://gatk.broadinstitute.org/>). Single nucleotide variants (SNVs) and small insertions and deletions (indels) were called and filtered using GATK Mutect2 and FilterMutectCalls with recommended parameters, and annotated with SnpEff (4.3, Pablo Cingolani, <https://pcingola.github.io/SnpEff/>). To compile a list of genes with possible involvement in BL pathophysiology, we took the union of: COSMIC (Wellcome Sanger Institute, Hinxton, UK, <https://cancer.sanger.ac.uk/cosmic>) 'Genes with mutations' for BL histology, genes mutated in the validation cohort of Grande et al.¹⁸ and recurrently mutated genes from the Love et al.¹⁶ cohort, yielding 4 272 genes. To enrich for functional variants, intergenic, intronic, and synonymous SNVs were excluded. To avoid including potential germline variants, variant allele frequencies (VAFs) in the range (0, 0.97) were included. Data visualisation and statistical analysis was performed in R: The R Project for Statistical Computing (<https://www.r-project.org/>).

RT-qPCR quantification of gene expression

All kits were used according to the manufacturer's instructions. To compare gene expression levels, total RNA was isolated with the RNeasy Plus Mini Kit (Qiagen) before RNA (1 μ g) was reverse transcribed using the ProtoScript II First Strand cDNA Synthesis Kit (NEB, Ipswich, MA, USA). RT reactions were diluted (1:10) and 10 ng equivalent (to input RNA amount) was used as the template DNA for quantitative polymerase chain reaction (qPCR) using Power SYBR Green PCR Master Mix (ThermoFisher) with standard reaction conditions on the QuantStudioTM 6 Flex Real-Time

Table I. Details of biopsy site, diagnosis, disease stage and engraftment status for each patient sample and the resulting patient-derived xenograft (PDX).

Sample number	Patient	Biopsy site	Diagnosis	Stage	Engraftment success	PDX formed
1	1	Needle biopsy of abdominal mass	Burkitt lymphoma	III	No	
2	1	Bone marrow	Burkitt lymphoma	III	No	
3	2	Pleural effusion	Burkitt lymphoma	III	Yes	PDX1
4	3	Peripheral blood	Burkitt lymphoma/leukaemia with CNS involvement	IV	Yes	PDX2
5	3	Bone marrow	Burkitt lymphoma/leukaemia with CNS involvement	IV	No	
6	4	Peripheral blood	Burkitt lymphoma	IV	No	
7	4	Bone marrow	Burkitt lymphoma	IV	No	
8	5	Bone marrow	Burkitt lymphoma/leukaemia	IV	No	
9	6	Bone marrow	Burkitt lymphoma	III	Yes	PDX3
10	7	Pleural effusion	Burkitt lymphoma	III	Yes	PDX4
11	8	Pleural effusion	Burkitt lymphoma	IV	Yes	PDX5
12	9	Peripheral blood	Burkitt lymphoma	IV	No	
13	9	Bone marrow	Burkitt lymphoma	IV	No	
14	10	Peritoneal effusion	Burkitt lymphoma	Relapse	Yes	PDX6

All samples were received following procedure to obtain diagnostic biopsies prior to treatment except for sample 14 from patient 10 that was taken when the patient had relapsed and was refractory to therapy with ICE (ifosfamide, carboplatin, etoposide). CNS, central nervous system.

PCR System (ThermoFisher). PCR was carried out using primers specific to the following genes: *MYC* FWD 5'-GGCT CCTGGCAAAAGGTCA-3', *MYC* R 5'-CTGCGTAGTTGT GCTGATGT-3'; *BCL2* FWD 5'-GGTGGGGTCATGTGTG TGG-3', *BCL2* R 5'-CGGTTTCAGGTAAGTCAATCC-3'; *BCL6* FWD 5'-ACACATCTCGGCTCAATTTGC-3', *BCL6* R 5'-AGTGTCCACAACATGCTCCAT-3'; *GNA13* FWD 5'-CCC AAGGAATGGTGAAACAA-3', *GNA13* R 5'-ACCCAGTT-GAAATTCTCGACG-3'; *ID3* FWD 5'-GAGAGGCACTCAG CTTAGCC-3', *ID3* R 5'-TCCTTTTGTGCGTTGGAGATGAC-3'; *TCF3* FWD 5'-CCGACTCCTACAGTGGGCTA-3', *TCF3* R 5'-CGCTGACGTGTTCTCCTCG-3'; *PIM1* FWD 5'-GAG AAGGACCGGATTTCCGAC-3', *PIM1* R 5'-CAGTCCAG-GAGCCTAATGACG-3'; *ARID1A* FWD 5'-CCAGCAGAA CTCTCAGACC-3', *ARID1A* R 5'-CTGAGCGAAGGAC GAAGACG-3'; *CDK4* FWD 5'-ATGGCTACCTCTCGATAT-GAGC-3', *CDK4* R 5'-CATTGGGGACTCTCACACTCT-3'; *CDC7* FWD 5'-AGTGCCTAACAGTGGCTGG-3', *CDC7* R 5'-CACGGTGAACAATACCAAATGA-3'; *GAPDH* FWD 5'-GGAGCGAGATCCCTCCAAAAT-3', *GAPDH* R 5'-GGC

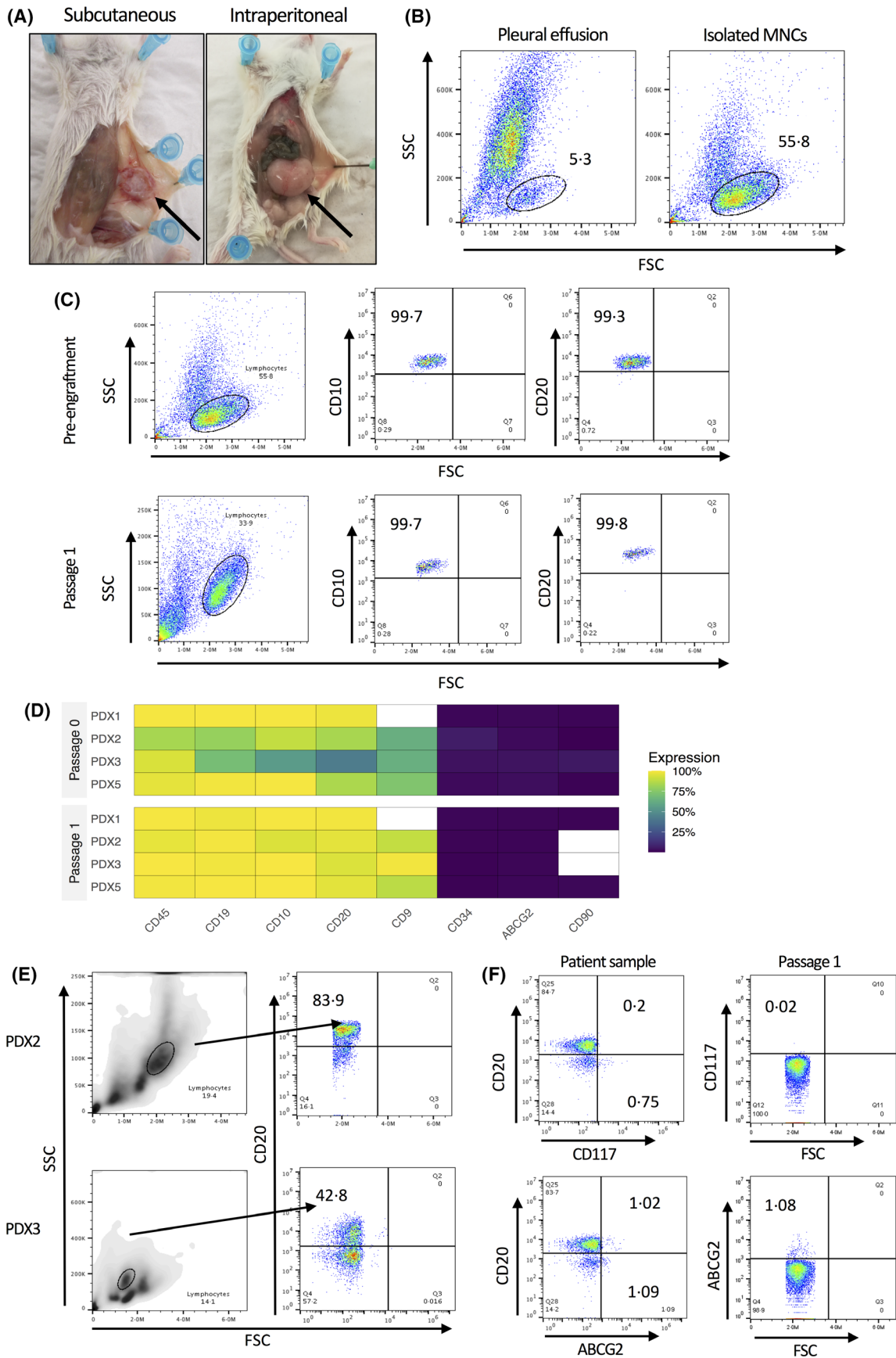
TGTTGTCATACTTCTCATGG-3'; *PTEN* FWD 5'-TTTGAA-GACCATAACCCACCAC-3', *PTEN* R 5'-ATTACACCAG TTCGTCCCTTTC-3'; *PAX5* FWD 5'-ACTTGCTCATCAA GGTGTCAG-3', *PAX5* R 5'-TCCTCCAATTACCCCAGGC TT-3'; *MTOR* FWD 5'-TCCGAGAGATGAGTCAAGAGG-3', *MTOR* R 5'-CACCTTCCACTCCTATGAGGC-3'; *SMARCA4* FWD 5'-GACCAGCACTCCCAAGTTAC-3', *SMARCA4* R 5'-CTGGCCCCGGAAGACATCTG-3'. Data were analysed using the double delta Ct ($\Delta\Delta$ Ct) method conducted with normalization to *GAPDH* (Δ Ct) before relative expression level comparison to the control sample ($\Delta\Delta$ Ct). All qPCR reactions were performed in technical triplicates.

Results

Establishment of PDX models from paediatric Burkitt lymphoma biopsy material

Samples from paediatric patients diagnosed with BL were taken from various sites including tumour biopsy ($n = 1$),

Fig 1. Tumour cell characteristics are maintained following engraftment in NSG mice. (A) Mononuclear cells (MNCs) were isolated from a patient pleural effusion sample and resuspended in phosphate-buffered saline (PBS) before injection via the subcutaneous (left) or intraperitoneal route (right). (B) The lymphocyte population of patient sample 3 pleural effusion was analysed before and after gradient centrifugation and isolation of MNCs, resulting in enrichment of lymphocytes. (C) Isolated MNCs from patient sample 3 were analysed for surface antigen expression before and after engraftment in a mouse [patient-derived xenograft (PDX) 1]. (D) Overview of surface antigen expression before and after engraftment. Heatmap represents percentage surface antigen expression as determined by flow cytometry. (E) The tumourigenic cell population in a peripheral blood sample (patient sample 4, PDX2) and a bone marrow sample (patient sample 9, PDX3) were identified based on expression of CD20. (F) MNCs from initial peripheral blood biopsy sample of patient sample 4 and after passage 1 (PDX2) were analysed for expression of surface antigens CD117 and ABCG2. [Colour figure can be viewed at wileyonlinelibrary.com]



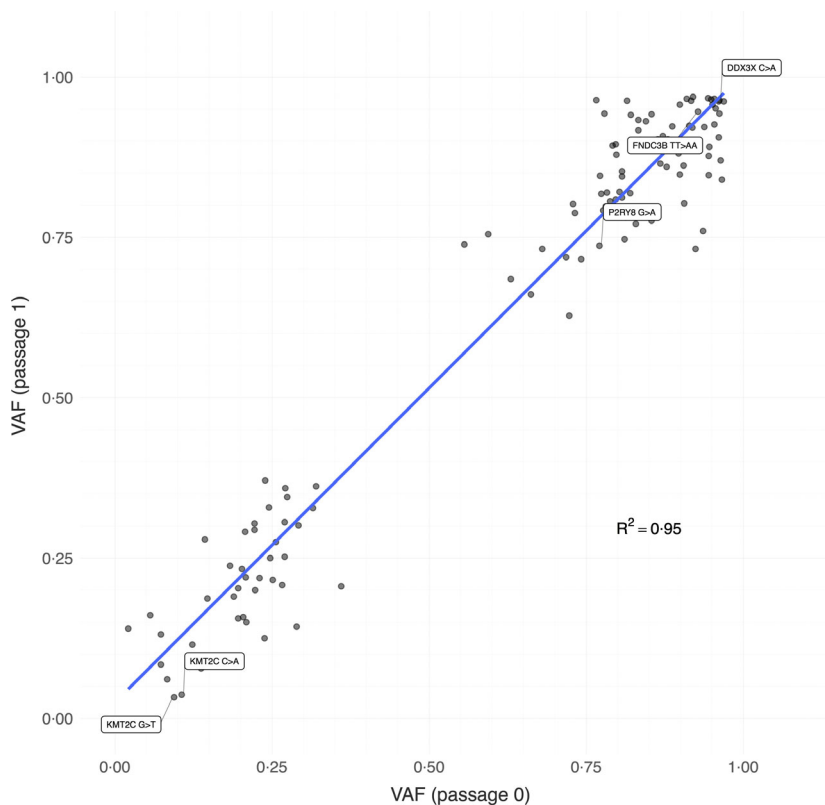


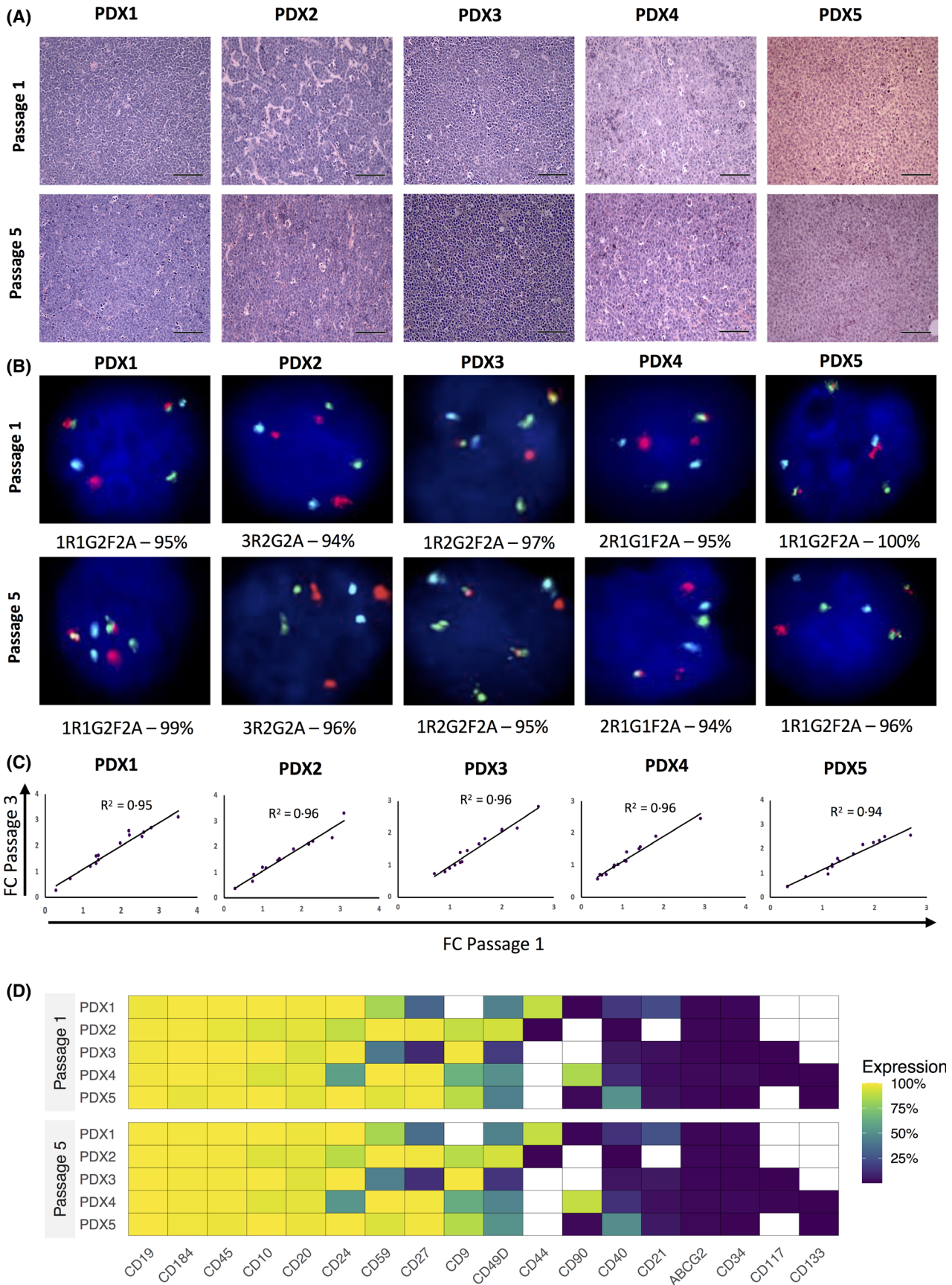
Fig 2. No new variants in Burkitt lymphoma (BL)-related genes emerged or were lost following expansion of a xenograft in NSG mice. Scatter plot of variant allele frequencies in a patient BL tumour before and after first passage in a mouse. Individual points represent Single nucleotide variants and small indels in genes previously reported to be mutated in BL; see Materials and methods for details. Mutated genes from the validation cohort of Grande et al.¹⁸ are highlighted. Blue line represents linear regression fit ($F_{1,117} = 2\,210$, $R^2 = 0.95$, $P = <2.2 \times 10^{-16}$). R^2 , adjusted R-squared statistic. [Colour figure can be viewed at wileyonlinelibrary.com]

peritoneal fluid ($n = 1$), pleural effusion ($n = 3$), bone marrow ($n = 6$) and peripheral blood ($n = 3$) (Table I). In total, 14 samples were obtained from 10 patients with six samples resulting in successful engraftment; an engraftment rate of 43%. The primary method of engraftment was subcutaneous (SC) injection of mononuclear cells (MNCs) with matrigel, although cells were also injected in separate mice intraperitoneally (IP) and intravenously (IV) when sufficient numbers were available. Of note, IV injection was attempted for all tumour samples from peripheral blood and bone marrow but no engraftment of Burkitt cells in the peripheral blood of mice was detected. In all cases where SC injection resulted in tumour engraftment, IP injection of cells from the same sample also successfully engrafted (Fig 1A). Pleural effusion samples engrafted most consistently with 3/3 forming a PDX

while 0/1 solid tumour, 1/1 peritoneal fluid, 1/3 peripheral blood and 1/6 bone marrow samples were successfully engrafted. The only sample of peritoneal fluid, also the only tumour from a relapse patient, was engrafted SC only and formed a tumour.

Given that all but one biopsy sample were obtained in liquid form from sites with potentially mixed cell populations, non-tumour cells were initially depleted from all peripheral blood, pleural effusion and bone marrow samples by gradient centrifugation. This resulted in an enrichment of lymphocytes including the B-cell tumour population. For example, lymphocytes increased from 5 to 55% of the cell population of the pleural effusion (Fig 1B) after MNC isolation of patient sample 3, the first sample to form a PDX. This enriched lymphocyte population was $CD10^+CD20^+$, a

Fig 3. Tumour histological, molecular and surface expression features were maintained through passage in NSG mice. (A) Representative haematoxylin–eosin (H&E) images of patient-derived xenograft (PDX) tumours at passage 1 and 5 taken from all five PDX models (scale bar = 100 μm). (B) fluorescence *in situ* hybridisation (FISH) analysis of tumour cells at passage 1 and 5 from all five PDX. A representative image of a 4',6-diamidino-2-phenylindole (DAPI)-stained nucleus is shown. Figures below the images represent the percentage of cells positive for the MYC translocation ($n = 100$). Aqua (A) signal = centromere of chromosome 8, red (R) signal = MYC, green (G) signal = IgH, F = fusion. (C) Quantitative real time- polymerase chain reaction (RT-qPCR) was carried out for a selection of 14 Burkitt lymphoma (BL) representative genes at passages 1 and 5 for all five PDX with cDNA from the Raji cell line as the control. (D) Detailed surface expression profiling of each PDX highlights the significant inter- and intratumour heterogeneity and maintenance from P1 to P5. Heatmap represents percentage surface antigen expression as determined by flow cytometry; white represents antigen not expressed in that PDX. [Colour figure can be viewed at wileyonlinelibrary.com]



phenotype characteristic of Burkitt lymphoma cells (Fig 1C). Importantly, the cell surface phenotype of the PDX1 cell population after passage 1 was indistinguishable from that of the lymphocyte population of the pleural effusion biopsy sample from which it was derived (patient sample 3; Fig 1C, D). PDX5, also derived from a pleural effusion sample, showed similar maintenance of the lymphocyte cell surface phenotype between biopsy and passage 1 (Fig 1D). PDX2 and PDX3 were derived from peripheral blood and bone marrow patient samples, respectively, with a mixed population of healthy and tumourigenic blood cells within the biopsy samples (Fig 1E). Once the PDX had been established, that is, tumours grew in the mice on first passage, 96% of lymphocytes in PDX2 and 95% in PDX3 were CD20⁺, compared to 84% and 42% of the total lymphocyte population, respectively, in the original patient biopsies, suggesting that tumour cells are selected *in vivo* (Fig 1D,E). Conversely, the small population of CD117⁺ cells present in the starting material for PDX2 was lost in the established graft, although these cells were CD20⁻ suggesting they were not tumour cells (Fig 1F). However, a minor population of CD20⁺ABCG2⁺ cells was present in the initial biopsy and in the established graft, suggesting that even minor cell populations within the patient biopsy sample were maintained in the PDX on engraftment (Fig 1F). PDX4 did not have spare biopsy material available for analysis.

To investigate the maintenance of genetic intratumour heterogeneity in the PDX model employed in this study, WGS was performed on the PDX developed from a relapse BL peritoneal fluid sample that had sufficient material both at biopsy and after passage 1 (PDX6). Importantly, no new variants in BL-related genes emerged or were lost following expansion of the xenograft *in vivo* (Fig 2; Figure S1). Furthermore, linear regression of VAFs before and after passage yielded an adjusted R^2 statistic of 0.95, indicating a good fit (slope: 0.98, intercept: 0.03, $P < 2.2 \times 10^{-16}$).

PDX models maintain their phenotypic, molecular and histopathological features through passage

To validate that PDX models are a robust and reliable resource that recapitulate the features of paediatric BL through propagation in mice, tumours were monitored at each passage. Histopathological analysis of each tumour after

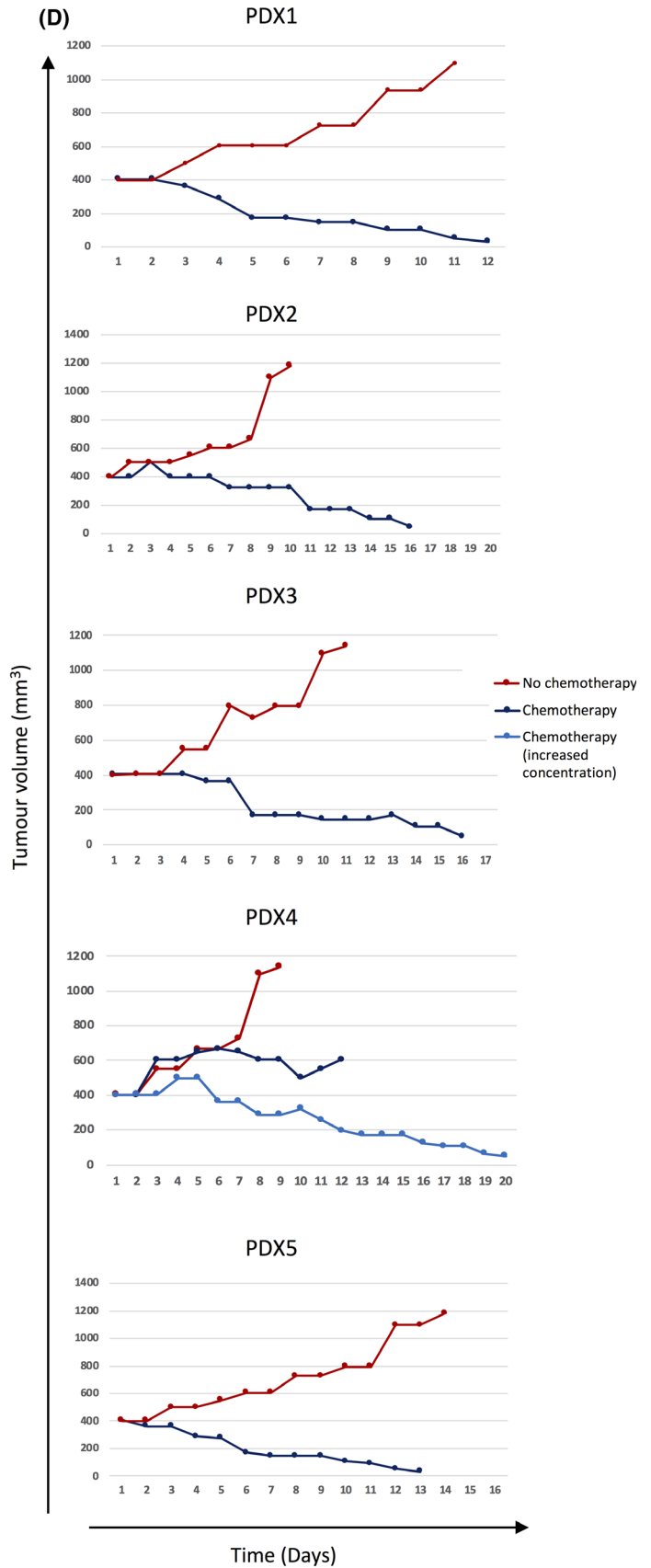
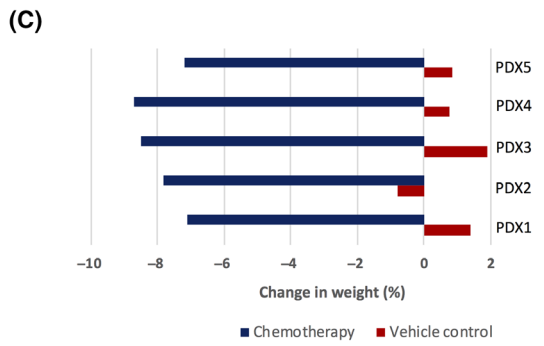
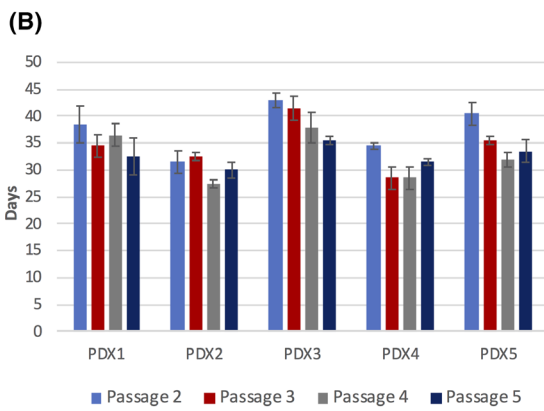
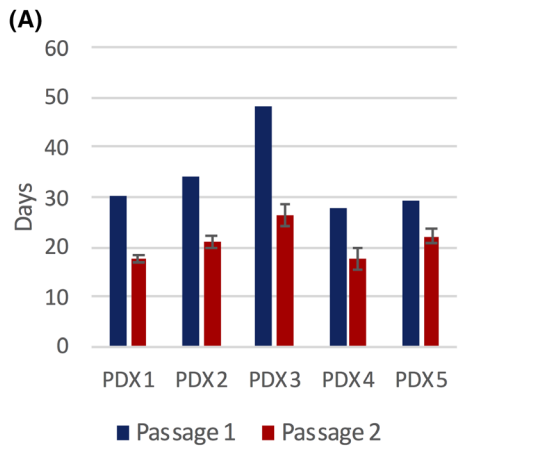
passages 1 (P1) and 5 (P5) was performed showing maintenance of high-grade lymphoma histology (Fig 3A). The characteristic *MYC* translocation of BL was identified at diagnosis for each patient and maintenance of the translocation signal in all PDX cells was monitored through passage using FISH. At P5, for all of the PDX (PDX1–5), the specific *MYC* translocation was maintained in almost 100% of tumour cells (Fig 3B). To determine if serial passage impacts the expression profile of tumours, expression profiling of genes associated with BL was conducted at P1 and P5. The coefficient of determination between P1 and P5 for each PDX was greater than 0.94, highlighting consistent expression levels of this limited selection of genes at both passages (Fig 3C; Figure S2). Comparison with the original diagnostic material was not possible, as there was insufficient material available.

Cell surface expression profiling between passages 1 and 5 also highlighted that all tumours faithfully maintained their surface expression profile over passage. All five PDXs showed strong expression of surface proteins characteristic of BL, such as CD20⁺, while minor populations of tumour cells were also maintained within each PDX, for example, ABCG2⁺ cells (Fig 3D). This highlights the significant intra- and intertumour heterogeneity within these PDX models which was also maintained through multiple passage (Fig 3D). The maintenance of precise surface expression profiles within each PDX, over five passages, highlights the existence of an intricate population equilibrium within the individual tumours. Importantly, subpopulations that were maintained through passage, at varying levels in the five PDXs, included populations not commonly reported in BL such as CD9⁺, CD90⁺, CD44⁺ and CD49D⁺ cells (Fig 3D).

PDXs can be used to mimic response to therapy in vivo

The mean number of days for the injected primary cells to first produce palpable tumours when engrafted SC was 33 (range 28–48 days) with PDX3 from a bone marrow sample having the longest engraftment time (Fig 4A). Once established, passage 2 of each PDX led to the development of palpable tumours more quickly (Fig 4A) and the total time from injection to produce tumours of maximum allowed size, according to UK guidelines, was largely consistent for each PDX across passages, from P2 onwards (Fig 4B). The ability of these PDX models to give rise to large, palpable

Fig 4. Established patient-derived xenograft (PDX) models respond to multiagent chemotherapy with PDX4 showing greatest resistance. (A) The number of days for primary tumour samples to achieve initial engraftment (passage 1) and for subsequent PDXs to engraft at passage 2 was monitored. Graph shows $n = 1$ for passage 1 and means and standard deviation for passage 2, $n = 2$. (B) The number of days from injection of cells for PDX tumours to reach maximum size was monitored for PDXs at each passage. Graph shows means and standard deviation, $n = 2$. (C) The impact of treatment on animal weight was monitored after chemotherapy and vehicle control administration and maximum percentage change in weight recorded. (D) Chemotherapy was administered intraperitoneally to mice when tumours reached 400 mm³ in volume. Drug concentrations: 3 mg/kg doxorubicin, 15 mg/kg methotrexate, 0.25 mg/kg vincristine. Increased to 3.75 mg/kg doxorubicin, 18.75 mg/kg methotrexate, 0.3125 mg/kg vincristine in PDX4. Treatment was repeated every 72 h and ceased when tumour volume reached 50 mm³. Graphs show tumour volume measurements taken every day. Tumour volume was calculated using the modified ellipsoid formula $1/2(\text{Length} \times \text{Width}^2)$. [Colour figure can be viewed at wileyonlinelibrary.com]



tumours within a relatively short timeframe provides an excellent resource to conduct *in vivo* experiments and investigate patient-specific tumour characteristics, such as heterogeneity and response to therapy. Multi-agent chemotherapy (doxorubicin, methotrexate and vincristine) was administered every 72 h, once tumours reached a volume of 400 mm³. Chemotherapy was stopped after a maximum of six doses when tumours shrank to 50 mm³. Chemotherapy led to a discrete but significant weight loss for all 5 PDX models compared to vehicle-only controls (Fig 4C). In the case of PDX 1, 2, 3 and 5, tumours responded to lower-dose chemotherapy based on decreased tumour volumes (Fig 4D), whereas PDX4 only showed a significant treatment response upon administration of an increased concentration of multi-agent chemotherapy.

Discussion

Survival rates in paediatric BL approach 90% but salvage options in relapse and refractory disease remain very limited.⁵ It is necessary for us to develop a greater understanding of the different populations within tumours to reduce the use of toxic chemotherapy and to develop targeted therapies for difficult-to-treat chemoresistant relapse and refractory cases. In evidence, studies have shown that personalised therapeutic approaches designed according to PDX treatment responses result in improved clinical outcomes.¹⁹ For adult B-NHL, due to the genetic heterogeneity of tumours, several different pathways leading to drug resistance have been identified and this is also likely the case for paediatric BL. Chemoresistance in paediatric BL may, therefore, require the development of personalised approaches to address patient-to-patient genetic heterogeneity. In this study we have successfully established PDX models of paediatric BL and demonstrated their ability to faithfully maintain molecular and phenotypic characteristics through multiple passages. This ensures the model possesses a high level of clinical relevance and can be used for identifying populations with chemoresistance potential as well as to investigate the potential efficacy of targeted therapies.

Patients in this study presented with both BL and leukaemia and PDXs were mainly established from liquid biopsies from peripheral blood, bone marrow, pleural effusion and peritoneal fluid. The only solid biopsy sample included did not lead to PDX establishment. An engraftment rate of 43% was observed when considering all specimens received and each of the engrafted PDX were successfully propagated by long-term serial passage. This rate is comparable to that in many other similar studies with one review of existing data highlighting that engraftment rates typically vary between 23% and 75% depending on the tumour type²⁰: A study of adult B-NHL, including mainly mantle cell lymphoma (MCL) and DLBCL, with one BL sample had a 67% success rate for serial passage²¹ and a further study in DLBCL reported a 32% success rate for serial passage.¹⁷

Pleural effusion samples had the highest engraftment rate in this study, although one PDX developed from peripheral blood and another from bone marrow via both the IP and SC routes. In contrast, tumour growth was not observed, independent of the site of origin, when engrafted IV. Given these potential limitations, a key consideration when utilising PDXs as a model for cancer is to determine how well they represent the original patient disease. In this study, PDX models established from pleural effusions showed a strong phenotypic correlation with the biopsy material, likely because there are fewer non-tumourigenic immune cells in the pleural effusion compared to the peripheral blood and bone marrow. The change in cell surface phenotype of the lymphocyte population between the diagnostic biopsy and the first passage for PDX established from peripheral blood and bone marrow, is likely due to outgrowth of tumour cells in the mouse with loss of infiltrating immune and other cells. A number of further lines of evidence suggest that changes did not occur to the tumour populations between the initial biopsy and P1: All tumours were almost 100% *MYC* translocation-positive after P1, matching reports of the original biopsy samples and minor cell populations that were lost from the biopsy sample were shown to be CD20⁻ and hence, most likely healthy immune cells that fell into the same forward and side scatter gate as the BL cells. Insufficient biopsy material meant detailed genomic analysis was not possible for these PDX. However, PDX6 generated from the peritoneal fluid of a relapsed patient had sufficient pre-engraftment and P1 material available for WGS. Analysis of potential functional variants in 4 272 genes associated with BL pathophysiology highlighted that no new variants in BL-related genes emerged or were lost in the xenograft. Furthermore, linear regression analysis identified a strong relationship between VAF before and after engraftment, suggesting that the methodology used for the establishment of the PDX models in this study did not introduce strong selection bias. The stability of the genetic characteristics after engraftment in this PDX is encouraging given that Schmitz *et al.* highlighted that in xenografted leukaemia, changes in copy number alterations emerged in the majority of cases during the first passage in mice.²² Other studies have also shown the persistence of tumour characteristics upon *in vivo* passage including a study of MCL PDX which did not observe any genetic alterations in 1 212 cancer-associated genes after two passages.²¹ Furthermore in a study of adult DLBCL PDXs, a comparison of the mutant allele fraction in primary specimens and the associated PDXs indicated that these models retained the complex genetic signature of primary samples.¹⁷

Analysis of the *MYC* translocation between subsequent passages from P1 onwards in our PDXs showed maintenance of the translocation in all cells at P5. Furthermore, the coefficient of determination for gene expression levels between P1 and P5 was greater than 0.94 for all five PDXs. At the cellular level, the histology of each tumour was maintained over five passages and, significantly, the heterogeneous surface

protein expression profile was also highly conserved, highlighting the potential importance of a tightly controlled population equilibrium within the tumours. Following initial engraftment these PDX models consistently produce large tumours within 4–6 weeks and provide an excellent resource to investigate the functional significance of tumour heterogeneity. The response of each PDX to doxorubicin, methotrexate and vincristine, components of the LMB chemotherapeutic backbone for paediatric BL patients, is also encouraging and highlights that they can be used to model therapy response and perhaps to elucidate causes of resistance. Of note, differential sensitivity to chemotherapy was observed among PDXs in this study, highlighting the importance of intertumour heterogeneity in evaluating treatment response and the need for personalised medicine approaches.

In summary, we describe in the largest cohort of BL PDX, based on phenotypical and in-depth molecular characterisation, the persistence of BL characteristics upon serial passaging in mice. These PDX models provide a valuable resource to investigate the functional and clinical significance of the heterogenous populations in BL. These models may be used to elucidate mechanisms of resistance and relapse so we can ultimately improve the dismal prognosis for this patient population.

Acknowledgements

We are grateful to Dave, Nic, Brenda and Matt for their support, courage and determination to put an end to childhood cancer in memory of Alex. SF, JDM, GAAB and SDT are supported with funding from the Alex Hulme Foundation. We thank the Cambridge NIHR BRC Cell Phenotyping Hub, Addenbrooke's Hospital, Cambridge; Central Biomedical Services (CBS), Addenbrooke's Hospital, Cambridge; Haematopathology and Oncology Diagnostic Service (HODS) Lab, Addenbrooke's Hospital, Cambridge; and the Histology Lab, Department of Pathology, University of Cambridge. We are also extremely grateful to all the children and their parents who donated their tumour tissues for this study.

Author contributions

Conceptualization: SF, GAAB, SDT; methodology: SF, JDM and SDT; investigation: SF, JDM, OG, LJ, TIMM; writing — original draft: SF and SDT; writing — review and editing: SF, GAAB, JDM, NP, LK, SDT; writing — final approval: all; funding acquisition: SDT; resources: NB, SB, SDT, AO'M, OS; supervision: SDT, GAAB.

Supporting Information

Additional supporting information may be found online in the Supporting Information section at the end of the article.

Fig S1. Bland–Altman plot with marginal histograms.

Fig S2. Bland–Altman plots for patient-derived xenografts (PDXs) 1–5.

References

- Sandlund JT, Downing JR, Crist WM. Non-Hodgkin's lymphoma in childhood. *N Engl J Med.* 1996;**334**:1238–48.
- Burkhardt B, Zimmermann M, Oshlies I, Niggli F, Mann G, Parwaresch R, et al. The impact of age and gender on biology, clinical features and treatment outcome of non-Hodgkin lymphoma in childhood and adolescence. *Br J Haematol.* 2005;**131**:39–49.
- Hochberg J, Waxman IM, Kelly KM, Morris E, Cairo MS. Adolescent non-Hodgkin lymphoma and Hodgkin lymphoma: state of the science. *Br J Haematol.* 2009;**144**:24–40.
- Hecht JL, Aster JC. Molecular biology of Burkitt's lymphoma. *J Clin Oncol.* 2000;**18**:3707–21.
- El-Mallawany NK, Cairo MS. Advances in the diagnosis and treatment of childhood and adolescent B-cell non-Hodgkin lymphoma. *Clin Adv Hematol Oncol.* 2015;**13**:113–23.
- Minard-Colin V, Brugières L, Reiter A, Cairo MS, Gross TG, Woessmann W, et al. Non-Hodgkin lymphoma in children and adolescents: progress through effective collaboration, current knowledge, and challenges ahead. *J Clin Oncol.* 2015;**33**:2963–74.
- Woessmann W, Seidemann K, Mann G, Zimmermann M, Burkhardt B, Oshlies I, et al. The impact of the methotrexate administration schedule and dose in the treatment of children and adolescents with B-cell neoplasms: a report of the BFM Group Study NHL-BFM95. *Blood.* 2005;**105**:948–58.
- Patte C, Auperin A, Gerrard M, Michon J, Pinkerton R, Spoto R, et al. Results of the randomized international FAB/LMB96 trial for intermediate risk B-cell non-Hodgkin's lymphoma in children and adolescents: it is possible to reduce treatment for the early responding patients. *Blood.* 2006;**109**:2773–80.
- Perkins SL, Lones MA, Davenport V, Cairo MS. B-Cell non-Hodgkin's lymphoma in children and adolescents: surface antigen expression and clinical implications for future targeted bioimmature therapy: a children's cancer group report. *Clin Adv Hematol Oncol.* 2003;**1**:314–7.
- Minard-Colin V, Aupérin A, Pillon M, Burke GAA, Barkauskas DA, Wheatley K, et al. Rituximab for high-risk, mature B-cell non-Hodgkin's lymphoma in children. *N Engl J Med.* 2020;**382**:2207–19.
- Griffin TC, Weitzman S, Weinstein H, Chang M, Cairo M, Hutchison R, et al. A study of rituximab and ifosfamide, carboplatin, and etoposide chemotherapy in children with recurrent/refractory B-cell (CD20+) non-Hodgkin lymphoma and mature B-cell acute lymphoblastic leukemia: a report from the Children's Oncology Group. *Pediatr Blood Cancer.* 2009;**52**:177–81.
- Cairo M, Auperin A, Perkins SL, Pinkerton R, Harrison L, Goldman S, et al. Overall survival of children and adolescents with mature B cell non-Hodgkin lymphoma who had refractory or relapsed disease during or after treatment with FAB/LMB 96: a report from the FAB/LMB 96 study group. *Br J Haematol.* 2018;**182**:859–69.
- Pearson ADJ, Scobie N, Norga K, Ligas F, Chiodini D, Burke A, et al. ACCELERATE and European Medicine Agency Paediatric Strategy Forum for medicinal product development for mature B-cell malignancies in children. *Eur J Cancer.* 2019;**110**:74–85.
- Lee S, Day NS, Miles RR, Perkins SL, Lim MS, Ayello J, et al. Comparative genomic expression signatures of signal transduction pathways and targets in paediatric Burkitt lymphoma: a Children's Oncology Group report. *Br J Haematol.* 2017;**177**:601–11.
- Derenzini E, Iacobucci I, Agostinelli C, Imbrogno E, Storlazzi CT, L'Abbate A, et al. Therapeutic implications of intratumour heterogeneity for TP53 mutational status in Burkitt lymphoma. *Exp Hematol Oncol.* 2015;**4**:24.
- Love C, Sun Z, Jima D, Li G, Zhang J, Miles R, et al. The genetic landscape of mutations in Burkitt lymphoma. *Nat Genet.* 2012;**44**:1321–5.

17. Chapuy B, Cheng H, Watahiki A, Ducar MD, Tan Y, Chen L, et al. Diffuse large B-cell lymphoma patient-derived xenograft models capture the molecular and biological heterogeneity of the disease. *Blood*. 2016;**127**:2203–13.
18. Grande BM, Gerhard DS, Jiang A, Griner NB, Abramson JS, Alexander TB, et al. Genome-wide discovery of somatic coding and noncoding mutations in pediatric endemic and sporadic Burkitt lymphoma. *Blood*. 2019;**133**:1313–24.
19. Hidalgo M, Bruckheimer E, Rajeshkumar NV, Garrido-Laguna I, De Oliveira E, Rubio-Viqueira B, et al. A pilot clinical study of treatment guided by personalized tumorgrafts in patients with advanced cancer. *Mol Cancer Ther*. 2011;**10**:1311–6.
20. Siolas D, Hannon GJ. Patient-derived tumor xenografts: transforming clinical samples into mouse models. *Cancer Res*. 2013;**73**:5315–9.
21. Zhang L, Nomie K, Zhang H, Bell T, Pham L, Kadri S, et al. B-cell lymphoma patient-derived xenograft models enable drug discovery and are a platform for personalized therapy. *Clin Cancer Res*. 2017;**23**:4212–23.
22. Schmitz M, Breithaupt P, Scheidegger N, Cario G, Bonapace L, Meissner B, et al. Xenografts of highly resistant leukemia recapitulate the clonal composition of the leukemogenic compartment. *Blood*. 2011;**118**:1854–64.